

---

# Characterization of significant molecular determinants of virulence of Enterovirus 71 sub-genotype B4 in Rhabdomyosarcoma cells

Pinn Tsin Isabel Yee<sup>a</sup>, Reham Ahmed Hashim Mohamed<sup>b</sup>, Seng-Kai Ong<sup>b</sup>, Kuan Onn Tan<sup>b</sup>, Chit Laa Poh<sup>a,\*</sup>

<sup>a</sup> Research Centre for Biomedical Sciences, School of Science and Technology, Sunway University, Kuala Lumpur, Selangor 47500, Malaysia; [isabely@sunway.edu.my](mailto:isabely@sunway.edu.my).

<sup>b</sup> School of Science and Technology, Department of Biological Sciences, School of Science and Technology, Sunway University, Kuala Lumpur, Selangor 47500, Malaysia.

**\*Corresponding Author:** Chit Laa Poh, Sunway University; [pohcl@sunway.edu.my](mailto:pohcl@sunway.edu.my)

**Emails of authors:** [isabely@sunway.edu.my](mailto:isabely@sunway.edu.my), [rihoahmed93@gmail.com](mailto:rihoahmed93@gmail.com); [ongsk@sunway.edu.my](mailto:ongsk@sunway.edu.my); [jefft@sunway.edu.my](mailto:jefft@sunway.edu.my).

## Abstract

One of the leading causes of the hand, foot and mouth disease (HFMD) is Enterovirus 71 (EV-A71), displaying symptoms such as fever and ulcers in children but some strains can produce cardiopulmonary oedema which leads to death. There is no FDA-approved vaccine for prevention of severe HFMD. The molecular determinants of virulence for EV-A71 are unclear. It could be a single or a combination of amino acids that determines virulence in different EV-A71 genotype/sub-genotypes. Several EV-A71 strains bearing single nucleotide (nt) mutations were constructed and the contribution of each mutation to virulence was evaluated. The nt(s) that contributed to significant reduction in virulence *in vitro* were selected and each mutation was introduced separately into the genome to construct the multiply mutated EV-A71 strain (MMS) which carried six substitutions of nt(s) at the 5'-NTR (U700C), VP1-145 (E to G), VP1-98E, VP1-244K and G64R in the vaccine seed strain that had a partial deletion within the 5'-NTR region (nt. 475-485) of  $\Delta 11\text{bp}$ . In comparison to the wild type strain, the MMS showed low virulence as it produced very low RNA copy number, plaque count, VP1 and had 10<sup>5</sup>-fold higher TCID<sub>50</sub>, indicative of a promising LAV candidate that should be further evaluated *in vivo*.

**Keywords:** enterovirus 71; hand foot mouth disease; virulence; vaccines; codon deoptimization; mutations.

## **Abbreviations**

EV-A71: Enterovirus 71; PV: Poliovirus; 5'-NTR: 5'- non translated region; aa: amino acid; nt: nucleotide; CPE: cytopathic effects; MOI: multiplicity of infection; RD: Rhabdomyosarcoma; PFU: plaque forming units; TCID<sub>50</sub>: 50% tissue culture infectious dose; VP1: Viral protein; LAV: live attenuated vaccine; MMS: multiply mutated strain.

## **1. Introduction**

In 2016, there were approximately 2.14 million reported cases of Hand, Foot and Mouth Disease (HFMD), including 204 deaths in China (WHO Western Pacific Region Surveillance Summary 2016). Vaccines against the Hand, Foot and Mouth Disease (HFMD) are highly desirable as HFMD has evolved to become a severe global and life threatening disease, ravaging lives of young children in cyclical epidemics in the Asia Pacific. With rising concern about the virulence of EV-A71, there is an urgent need for a vaccine against EV-A71 to be produced that is endorsed by the United States Food and Drug Administration (FDA). Up to date, several biopharmaceutical companies in China have ended their Phase III Clinical Trials, producing the inactivated vaccine (IV) adjuvanted with alum, against the sub-genotype C4a. Although the efficacy of their IVs was more than 90% against mild HFMD, it only conferred 80% protection against severe HFMD (Chong et al., 2015). The IV induces good humoral immunity but is deficient in the cellular arm of immunity, which is needed for long-term protection. Therefore, there is a need to develop other types of vaccines. The development of live attenuated vaccines (LAVs) is desirable as it is known to induce excellent immunogenicity, can elicit both

humoral and cellular immunity and able to confer live-long immunity. A LAV from the BrCr strain (S1-3') prototype strain carrying mutations in the 3'-NTR, 3D<sup>pol</sup> and 5'-NTR was constructed by Arita et al. (2007). Although there was reduced virulence, mild neurological symptoms were still observed in the 3 cynomolgus monkeys immunized with the EV-A71 (S1-3') strain. Hence, the plan to use this strain as a LAV was discontinued (Arita et al., 2007).

Before an effective LAV can be developed, there is a need to identify the genetic determinants of virulence. Once the specific determinants of virulence in EV-A71 have been identified, rational design of the LAV can be carried out by site directed mutagenesis (SDM) to target the specific amino acids that are associated with virulence. Classification of genetic determinants of virulence in EV-A71 by analyzing differences in the genome has been published. Sequence comparison between virulent and non-virulent strains showed that 4 amino acids (aa) in VP1 (Gly<sup>P710</sup>/Gln<sup>P710</sup>/Arg<sup>P710</sup>/Glu<sup>P729</sup>), 1 aa. in the 2A protein (Lys<sup>P930</sup>) and 4 nucleotides (nt) in the 5'-NTR (G<sup>P272</sup>, U<sup>P488</sup> and A<sup>P700</sup>/U<sup>P700</sup>) could be genetic determinants for virulent EV-A71 sub-genotype C4 strains (Li et al., 2011). In addition, it was postulated that the EV-A71 mutant displaying high-fidelity (sub-genotype B4) with a single aa. change, (G64R) in its RNA-dependent RNA polymerase (RdRP) enzyme greatly reduced viral pathogenicity *in vivo* (Meng and Kwang, 2014). Kataoka et al. (2015) found that if the aa. glutamic acid was present at position 145 of VP1 (VP1-145E) in EV-A71 (sub-genotype C1), the virus induced neuro-pathogenesis and viremia more efficiently in cynomolgus monkeys than if glycine (G) was found at residue 145 (VP1-145G) (Kataoka et al., 2015).

The analysis of significant molecular determinants of virulence that were responsible for the attenuated phenotypes of the Sabin Oral Polio Vaccine (OPV) strains was due to the complete sequences of 3 poliovirus (PV) genomes and the development of infectious PV cDNA clones. For example, the Sabin 1 strain differed from its wild type strain with 57 nt. substitutions (Nomoto et al., 1982). It was found that the A480G in the IRES region is the most vital determinant of virulence that contributed to the attenuation in the Sabin 1 strain. It could be possible that nt. 480 affects the formation of a structure in the 5'-NTR responsible for neuro-virulence (Kawamura et al., 1989). For the Sabin 2 strain there were only 2 nt. substitutions (nt. 481 in IRES and nt. 2909 in VP1), whereas a total of 10 nt. substitutions were discovered for the Sabin 3 strain. Amongst the 10, there were 3 significant molecular determinants of virulence (C274U in IRES, C2034U in VP3, and U2493C in VP1 (Chia et al., 2014; Huang et al., 2013; Westrop et al., 1989). Virulent strains of EV-A71 are referred to as the new polio as it is neurotropic. Both the enteroviruses share very high sequence homology, particularly in the 5'-NTR. EV-A71 contains a similar nt. G481 that is a significant molecular determinant of neuro-virulence in the PV wild type. Hence, studies on PV in earlier research could be good references to design attenuated EV-A71 viruses.

With advances in molecular biology, novel approaches to viral attenuation can be further studied such as altered replication fidelity and codon de-optimization. As high mutation rates often hinder the effectiveness of a LAV, increasing the replication fidelity can potentially attenuate whole virus population, culminating to a population collapse with the absence of mutating vital immunogenic epitopes. For all species, codon pair usage is biased and some codon pairs are utilized more often than others (Gutman and Hatfield, 1989). A big part of the genetic code is redundant as contiguous pairs of aa. can be coded

for by 36 alternate pairs of synonymous codons (Buchan et al., 2006; Sharp et al., 1986). Through the substitution of alternate but synonymous codons within the genome sequence, this would produce different codon pairs but expressing a similar sequence of amino acids. The proteins expressed from these viruses would elicit the same immune response as the wild type viruses. Burns et al. (2006) replaced half of the total codons in the Sabin type 2 OPV strain (within capsid region) with less frequently utilized synonymous codons. They discovered that processing and manufacturing of viral proteins were unaffected but viral fitness was reduced (Burns et al., 2006). Subsequently, they replaced natural capsid region codons with synonymous codons that had an abundance of CpG and UpA dinucleotides. Codon-deoptimized PVs were produced and these viruses had significantly lower overall fitness as indicated by lower viral plaque number and virus yields (Burns et al., 2009).

Mueller et al. (2006) introduced the biggest number of less frequently utilized synonymous codons in the capsid region of PV type 1 Mahoney. They found a significant decrease in replicative fitness and number of infectious viral progeny. As compared to the wild type, there was also reduction in the viral infectivity up to approximately 1,000-fold and decrease in genome translation (Mueller et al., 2006). The codon deoptimized viruses remained attenuated after repeated cell passages and were genetically stable with minimal risk of reversion (Burns et al., 2006; Mueller et al., 2006). As these viruses have sequences that are fairly divergent from circulating wild type viruses, probabilities for further recombination and production of vaccine-derived variants will be reduced. In addition, the codon deoptimized attenuated viruses were genetically stable and showed low risk of reversion.

Previously, we had mutated the EV-A71 virus (sub-genotype B4 virus; 5865/Sin/000009) by substitutions at positions 475, 486, and 487 as these 3 nucleotides corresponded to the significant molecular determinants of neuro-virulence in PV Sabin strains 1, 2 and 3. In EV-A71, we have introduced a partial deletion (PD) (deletion from nt. 475-485 in the 5'-NTR) as it is considered to be genetically more stable than single site mutations. Compared to mutants with specific nt replacements at 475, 486 and 487, the EV-A71 PD mutant carrying the 11 base pair deletion demonstrated the lowest viral RNA copy number, plaque count and VP1 capsid protein. The PD mutant demonstrated low virulence and therefore, could possibly be a good potential seed strain for designing a LAV candidate (Yee et al., 2016).

In this study, we constructed several codon deoptimized EV-A71 viruses by substituting single synonymous codon at positions VP1 (98E), VP1 (242K), VP1 (244K), VP2 (149K) and 2A (930K) to assess the outcome of each codon deoptimization on replication fitness in Rhabdomyosarcoma (RD) cells. If the LAV has single site mutations, there is a strong possibility for reversion to occur. However, if it bears a short deletion and further mutations added to the genome, there is a possibility to reduce reversion and increase the stability of LAVs. In addition, a better attenuated mutant was constructed by introducing multiple mutations into the EV-A71 mutant PD. Hence, we also constructed a multiply mutated EV-A71 strain (MMS) by substituting 6 nucleotides at the 5'-NTR (U700C), VP1-145 (E to G), VP1 (98E), VP1 (242K), VP1 (244K), G64R in the mutant PD ( $\Delta$ 11bp in 5'-NTR). We evaluated the attenuation of virulence of the MMS in RD cells such as cytopathic effects, viral infectivity by tissue culture infectious dose (TCID<sub>50</sub>), plaque counts, production of VP1 and RNA copy number.

---

## 2. Materials and Methods

### 2.1 Tissue culture of RD cell line

Human Rhabdomyosarcoma cells (RD, ATCC # CCL-136) were propagated in Dulbecco's modified Eagle's Minimal Medium/F-12 (DMEM/F-12, Invitrogen, USA), that was supplemented with 1.5% NaHCO<sub>3</sub>, 10% fetal bovine serum (FBS) (Gibco, USA), 1% non-essential amino acids and 1% penicillin/streptomycin antibiotics. The cells were grown at 37°C in 5% CO<sub>2</sub> until they reached confluence.

### 2.2 Virus propagation and storage

A 75cm<sup>2</sup> tissue culture flask with 100% confluent Rhabdomyosarcoma (RD) cells was infected with 100 µl of virus supernatant. The flask was incubated for 1 h at 37°C and replaced with fresh DMEM supplemented with 2% FBS. The flask was incubated at 37°C for 24 - 48h and observed for cytopathic effects (CPE). The culture supernatants were harvested and freeze-thawed 3 times. The supernatants were then centrifuged at 10,000 x g for 20 minutes at 4°C to remove cell debris. The harvested supernatants were then stored at -80°C until further use.

### 2.3 Viral RNA Extraction

This process was performed using QIAamp® Viral RNA Mini Kit (Qiagen, Calif., USA). The principle was based on the selective binding properties of a silica-gel based membrane together with micro spin technology to extract viral RNA. The samples were lysed with a buffer which aids in denaturing RNases. The RNA was attached to the membrane which was then washed two times with buffers. The RNA was eluted with DEPC-treated water.

An aliquot of 140 µl taken from the samples were processed and the viral RNA was eluted in 50 µl of elution buffer (Qiagen, Calif., USA).

#### *2. 4 Reverse transcription of EV-A71 RNA*

The purified EV-A71 genomic RNA was converted into cDNA with the SuperScript® IV First Strand Synthesis System (ThermoFisher Scientific, Calif., USA). Each mixture contained 50 mM Tris-HCl (pH 8.3), 4 mM MgCl<sub>2</sub>, 10 mM DTT, 50 mM KCl, 0.5 mM dTTP, 0.4 MBq/mL [<sup>3</sup>H]-dTTP, 0.4 mM poly(A) oligo (dT)<sub>12-18</sub> and SuperScript® IV RT enzyme in 20 µL for 10 min at 37°C.

#### *2.5 Cloning of EV-A71 cDNA into the pCR-XL-TOPO vector*

The pCR-XL-TOPO vector was supplied with 3' thymidine (T) overhangs. The PCR products carrying 3' deoxyadenosine (A) overhangs were cloned in the pCR-XL-TOPO vector (Invitrogen, Calif., USA) based on the manual from the manufacturer. About 100 ng/µl of the cDNA template was prepared. An aliquot of 4 µl of the cDNA template in TE buffer was mixed with 1 µl (10 ng/µl) of plasmid DNA and incubated at room temperature for 30 min. Thereafter, 1 µl 6X TOPO stop solution was added to prevent the reaction from proceeding further. The recombinant pCR-XL-TOPO\_EV71 plasmid was then transformed into *E. coli* XL10-Gold® Ultra competent Cells (Invitrogen, Calif., USA).

#### *2.6 Site-directed mutagenesis*

Mutations were introduced by using the QuickChange Lightning Site-Directed Mutagenesis Kit (Agilent Technologies, Calif., USA). A pair of primers consisting the desired mutation was designed for the recombinant pCR-XL-TOPO\_EV71 vector. The cycling parameters



for the QuikChange Lightning Site-Directed Mutagenesis Method were: 95°C for 2 min for initial denaturation, followed by 18 cycles of 95°C for 20 secs, 60°C for 10 secs, 68°C for 5 min 30 sec and 68°C for 5 min for final elongation. Approximately 2 µl of *DpnI* enzyme was added to each amplification reaction to digest the non-mutated supercoiled dsDNA. The enzyme mix was transformed into XL10-Gold ultracompetent *E. coli* cells. Colonies were selected on LB + Kanamycin plate before 3 purified colonies were screened by sequencing.

### *2.7 Construction of a partial-deletion in the 5'-NTR of EV-A71*

A partial deletion (PD) (deletion from nt. 475-485 in the 5'-NTR) was constructed in the EV-A71 genome with a pair of 24-mer forward and 24-mer reverse primers. The mutation was introduced using the Q5® Site-Directed Mutagenesis Kit (New England Biolabs, USA) [(Chua et al., 2008)]. The presence of the deletion was confirmed using the nucleotide Basic Local Alignment Software (BLAST by NCIB).

### *2.8 Restriction digestion of plasmid DNA*

Digestion of pCR-XL-TOPO\_EV71 plasmid was carried out with restriction enzyme *EagI* (New England BioLabs, Massachusetts, USA). Briefly, this was carried out in an Eppendorf tube containing 15 µg of plasmid DNA, *EagI* in the corresponding 1X digestion buffer. All reactions were incubated for at least 2 hours at 37°C specified by the manufacturer.

### *2.9 Phenol-chloroform DNA purification*

The linearized DNA was added with an equal volume of phenol/chloroform/isoamyl alcohol (Invitrogen, Calif., USA) and subsequently, vortexed for 1 minute. Solvent and aqueous phases were visible after centrifugation at 15,000 x g for 10 minutes. The aqueous phase was aspirated and added with an equal volume of chloroform/isoamyl alcohol (Invitrogen, Calif., USA). This step was necessary to remove the remaining phenol. After 10 minutes of centrifugation at 15,000 x g, the aqueous phase was aspirated and 1/10 volume of 3 M sodium acetate (pH 5.2) was added and vortexed. An aliquot of 1 volume of isopropyl alcohol was added and kept at -20°C for 2 h. The precipitated DNA was centrifuged at 15,000 x g for 30 minutes at 4°C and the DNA pellet was rinsed with 70% ethanol. After air-drying, the pellet was dissolved with TE buffer and DNA concentration determined.

#### *2.10 In vitro transcription of SP6 promoter*

RNA transcription was performed utilizing the RiboMAX™ Large Scale RNA Production System-SP6 (Promega, Calif., USA). The reaction mixture was prepared in a 100 µl reaction volume according to the manufacturer's instructions. The reaction mixture was incubated at 37°C for 2 h, followed by addition of DNase for 30 minutes to remove parental DNA. The transcribed RNA was purified with the Illustra Microspin G-50 column (GE Healthcare Life Sciences, Chicago, USA) before transfection in RD cells (Han et al., 2010).

#### *2.11 Transfection of infectious RNA*

Overnight grown RD cells ( $1.5 \times 10^5$  cells/well in a 24-well plate) were prepared and used for transfection. Approximately 1 µg of RNA was transfected into a well within the 24-well plate. Prior to transfection, the growth medium was removed and replaced with Opti-MEM

(Invitrogen, Calif., USA). Transfection mix was prepared with a ratio of 2  $\mu$ l of Lipofectamine 2000 reagent to 1  $\mu$ g of RNA. The RNA-containing Opti-MEM was mixed with the Lipofectamine 2000 reagent containing Opti-MEM and incubated for 20 min at room temperature. Thereafter, the RNA-lipofectamine mixture was added to the RD cells drop-by-drop. Four hours after transfection, the transfection medium was removed and substituted with 500  $\mu$ L 10% FBS DMEM without Penicillin/Streptomycin.

#### *2.12 Quantitation of viral infectivity by tissue culture infectious dose (TCID<sub>50</sub>) assay*

RD cells ( $3.0 \times 10^4$  cells/well in a 96-well plate) were prepared a day before. Using DMEM serum-free media as a diluent, 10-fold serial dilutions of the harvested virus supernatant were carried out in quadruplicates in a 96-well plate. The negative control wells contained infected RD cells (without any virus supernatant). The plate was incubated at 37°C and observed daily for CPE for up to 48h.

#### *2.13 Viral RNA copy determination by real-time RT-PCR*

With the RNeasy extraction kit (Qiagen, Calif, USA), viral RNA was extracted from the virus suspension of transfected RD cells. Real-time PCR was carried out utilising the Touch™ Real-Time PCR Detection System (Bio-Rad, CFX96) and the SensiFAST™ Probe No-ROX One-Step Kit (BioLine, California, USA). The 20  $\mu$ l reaction mixture contained 4  $\mu$ l of RNA template, 10  $\mu$ l of 2x SensiFAST Probe No-ROX One Step Mix, 0.8  $\mu$ L forward and reverse primers (10 uM), 0.2  $\mu$ L probe (10 uM), 0.2  $\mu$ l reverse transcriptase enzyme, and 0.4  $\mu$ L RiboSafe RNase inhibitor. The reaction was performed for one cycle at 48°C for 10 min, 95°C for 2 min, followed by 40 cycles at 95°C for 5s and 60°C for 20s using 0.2 mL PCR tubes and caps (Bio-Rad, Calif, USA).

#### 2.14 VPI determination by western blot

Cellular proteins were extracted from harvested viral suspension of infected cells using RIPA lysis buffer (1.0% Triton X-100, 0.5% sodium deoxycholate, 0.1% sodium dodecyl sulfate, 50 mM Tris, pH 8.0, and protease inhibitor mixture). The protein samples were mixed with an equal volume of 4X SDS protein sample buffer (240 mM Tris-HCl, pH 6.8, 8% SDS, 5%  $\beta$ -mercaptoethanol, 40% glycerol and 0.04% bromophenol blue). The protein lysates were run on SDS-PAGE and transferred to nitrocellulose membrane (Millipore, Calif., USA). Thereafter, the membrane was blocked with 5% skim milk powder (Sigma-Aldrich, St Louis, USA) in Tris-Buffered Saline and Tween 20 (TBST) buffer for 1 h on an orbital shaker at room temperature. The membrane was then added with anti-enterovirus VP1 mouse monoclonal primary antibody (Merck, Calif., USA) diluted in 2.5% TBST overnight at 4°C. The next day the nitrocellulose membrane was washed three times with TBST, for 10 min each wash, prior to incubation with anti-mouse HRP secondary antibody (Sigma Aldrich, St Louis, USA) diluted in 2.5% TBST. After hybridization, the membranes were washed three times with TBST, for 10 min each wash, and then detected by chemiluminescence using ImageQuant (GE Healthcare Life Sciences, Calif., USA).

#### 2.15 Quantitation of viral titer by plaque assay

A 6-well plate with  $6 \times 10^5$  RD cells/well was seeded before viral infection the subsequent day. Serial 10-fold dilutions of viral suspension were prepared and 1 mL of each dilution was added to the cells for 1 h at 37°C. After viral attachment to the cells, the dilutions were aspirated and substituted with 2 mL of 0.9% w/v high viscosity carboxymethylcellulose (CMC) (Sigma Aldrich, St Louis, USA). After 48 h incubation, the CMC was removed and the cells were fixed with 10% formalin for 10 min. After fixation, the formalin was

removed and replaced with 0.5% crystal violet solution for 20 min incubation. The plaques were visible against a white background and the plaque forming units (PFU) were calculated for each EV-A71 mutant.

### *2.16 Bioinformatics Analysis*

The protein sequence of EV-A71 viral proteins was analyzed and the amino acid sequences were aligned with the Clustal method of DNASTAR MegAlign. Predictions of 5'NTR secondary structures of probable base pairs predictions, which might include pseudoknots was conducted by using databases such as RNA Structure at Rochester University: <http://rna.urmc.rochester.edu/RNAstructureWeb/index.html> and the mfold Web Server at [http://molbiol-tools.ca/RNA\\_analysis.htm](http://molbiol-tools.ca/RNA_analysis.htm).

### *2.17 Statistical Analysis*

Based on the data of at least three independent biological replicates, the mean  $\pm$  standard deviation was calculated. Statistical significance was determined with the Mann-Whitney test, whereby a p value of  $< 0.05$  was considered as statistically significant.

## **3. Results**

### *3.1.1 Cytopathic effects (CPE) caused by EV-A71 mutants*

The EV-A71 sub-genotype B4 virus (5865/Sin/000009) was genetically engineered to produce several codon deoptimised EV-A71 viruses by substituting single synonymous codon at positions VP1-98E, VP1-242K, VP1-244K, VP2-149K and 2A-930K. We also substituted several nucleotides (nt) at three positions within the 5'-NTR (C272U, U488C, U700C), VP1-E145G and the 3D<sup>pol</sup> region (G64R). The effects of these changes were

assessed by the inhibition of CPE in RD cells (Table 1). Upon transfection into RD cells with a multiplicity of infection (MOI) of 0.1, mutant C475U still caused the lowest CPE (Figure 1m) when compared to the wild type EV-A71 (Figure 1q). CPE was observed as round cells that lifted off the surface and there was abundant CPE observed with the EV-A71 wild type strain 41 (Figure 1q).

Mutant EV-A71 PD caused much lower CPE (Figure 1e) when compared to mutants C272U (Figure 1i) and 2A-930K (Figure 1h). Out of all the mutants, VP2-149K displayed abundant CPE (Figure 1g) as observed from the shrunken and rounding up of many RD cells. Mutants VP1-242K (Figure 1b), U488C (Figure 1j) and A486G (Figure 1n) demonstrated an intermediate amount of CPE after RD cell transfection. Based on the morphology shown in Figure 1c, 1f and 1o, infection of RD cells by mutants VP1-244K, VP1-E145G and G487A showed minimal CPE as cells had the healthy spindle-like shape of multiplying RD cells when compared to EV-A71 wild type sub-genotype B4 (Figure 1q). There were not many dead cells floating and showed similar morphology as the negative control (uninfected RD cells) (Figure 1p).

A multiply mutated EV-A71 strain (MMS) was constructed by substituting six nucleotides at the 5'-NTR (U700C), VP1-145 (E to G), VP1 (242K), VP1 (98E), VP1 (244K), G64R in the strain that consisted of a partial deletion in the 5'-NTR ( $\Delta$ 11bp). The MMS showed an absence of CPE (Figure 1l), displaying similar morphology as the negative control (Figure 1p). Lower CPE was observed in the MMS in comparison to the codon deoptimised mutant VP1-98E (Figure 1a) and G64R (3D<sup>pol</sup>) (Figure 1d). The morphology displayed by these EV-A71 mutants showed vast disparity from the abundant CPE observed for the positive control (wild type strain 41) (Figure 1q).

### 3.1.2. Quantitation of viral infectivity by tissue culture infectious dose (TCID<sub>50</sub>) assay

The tissue culture infectious dose (TCID<sub>50</sub>) is a measurement of the amount of virus that elicits cytopathic effect in 50% of the transfected cell cultures. The MMS demonstrated the highest TCID<sub>50</sub> of  $3.16 \times 10^8$  in comparison to the wild type EV-A71 strain ( $2.13 \times 10^3$ ) (Figure 2). This indicates that the MMS would need a significantly higher amount of virus ( $10^5$ -fold more) to elicit a cytopathic effect in 50% of the transfected cultures.

EV-A71 mutants VP1-E145G and VP1-244K also had  $10^5$ -fold increased TCID<sub>50</sub> value ( $3.16 \times 10^8$ ) in comparison to the positive control, indicative that the mutants showed a reduction in infectivity. EV-A71 mutants with SDM at VP1-242K ( $7.02 \times 10^5$ ) and G487A ( $7.50 \times 10^5$ ) demonstrated greater than  $10^2$ -fold rise in TCID<sub>50</sub> value in comparison to the positive control (EV-A71 wild type). EV-A71 mutant VP1-98E ( $1.16 \times 10^6$ ) and PD displayed  $10^3$ -fold increases in TCID<sub>50</sub> value in comparison to the wild type ( $2.13 \times 10^3$ ). An examination of the TCID<sub>50</sub> values implicates that mutants carrying single mutations in the VP1, for example, E145G and 244K as well as the MMS required the highest quantity of viruses to elicit cytopathic effect in 50% of the transfected cell cultures. The results indicated a high degree of attenuation in the two SDM mutants and the MMS carrying multiple mutations in its genome (Figure 2).

### 3.1.3 Viral RNA copy determination by real-time RT-PCR

Assays such as the viral RNA copy number quantitation and TCID<sub>50</sub> of various mutant strains will allow a better quantitative comparison of the growth aspects of the

different mutant strains. The viral RNA copy number of the EV-A71 mutant strains was assessed after transfection into RD cells. The positive control (wild type strain 41) produced the highest amount of viral RNA copy number ( $5.8 \times 10^4$ ). Significantly lower RNA copy numbers were detected for mutants C475U ( $1.02 \times 10^2$ ) and PD ( $1.05 \times 10^2$ ) (Figure 3). When the mutant strains were examined in RD cells, a few new mutations seem to decrease viral replication. It was demonstrated that mutant VP1-244K gave a yield of  $2.9 \times 10^2$  RNA copy number which was 100-times lesser than the positive control viral RNA copy number ( $5.8 \times 10^4$ ). It appeared that mutant VP2-149K yielded the greatest amount of viral RNA copy number of  $2.9 \times 10^4$  in comparison to the positive control (wild type strain 41). As the RNA copy number is still approximately half to that of the wild type strain, this shows that there remains some degree of attenuation.

In addition, the mutant VP1-E145G displayed significant decreases in viral RNA copy number ( $4.5 \times 10^2$ ) (Figure 3). The MMS yielded markedly low viral RNA copy number of  $1.3 \times 10^2$  and substantially decreased the viral RNA copy number to almost  $10^2$ -fold less in comparison to the positive control ( $5.8 \times 10^4$ ). A reduction of RNA copy number was also expressed by mutants VP1-98E and G64R (3D<sup>pol</sup>) at  $7.8 \times 10^2$  and  $1.4 \times 10^3$ , respectively.

### *3.1.4 VP1 determination by western blot*

Western blotting with monoclonal antibodies targeted at the VP1 capsid protein of EV-A71 could enable the detection of the viral capsid protein and be an indirect indicator of the ability of the various mutant strains to produce viable viral particles. Cellular protein



lysate was harvested from the supernatants of infected RD cells and sodium dodecyl sulfate polyacrylamide gel electrophoresis (SDS-PAGE) was performed to separate the EV-A71 proteins based on molecular weight (MW). A singular band was revealed at a MW of 37 kDa which corresponds to the VP1 monomer (Figure 4).

Based on the Western blot analysis, cellular proteins from RD cells transfected with the positive control (wild type EV-A71) (Figure 4, Lane 16) showed the greatest VP1 protein amount (36 kDa). There was hardly any VP1 observed for mutant C475U (Figure 4, Lane 8), mutant G487A (Figure 4, Lane 5) and mutant PD (Figure 4, Lane 13). The results were consistent with the cytopathic effect, TCID<sub>50</sub> infectivity and viral RNA copy number. There seems to be a few nt. in the EV-A71 viral genome that are attenuating the virus as the quantity of VP1 for some of the mutant strains were significantly lesser than the positive control (Figure 4, Lane 16). The mutant MMS (Figure 4, Lane 6), mutant VP1-244K (Figure 4, Lane 10) and mutant VP1-E145G (Figure 4, Lane 3) showed much lesser VP1 quantity in comparison to the positive control (wild type strain 41) (Figure 4, Lane 16). Although each mutant had caused significant reduction of virulence in terms of VP1, viral RNA copy number, and TCID<sub>50</sub> values, the introduction of all the mutations together in a single genome will enable increased genetic stability.

### *3.1.5 Quantitation of viral titre by plaque assay*

Plaque numbers produced by the different EV-A71 mutants were assessed in RD cells by plaque assays. Our objective is to evaluate the ability of the various mutants to

form plaques. RD cells infected with the positive control (wild type EV-A71 strain 41) gave the largest plaque number ( $8.0 \times 10^8$  PFU/mL). The smallest plaque numbers were produced by the MMS ( $1.2 \times 10^4$  PFU/mL) and mutant C475U ( $7.0 \times 10^4$  PFU/mL) (Figure 5).

Based on Figure 6, there are a few nt. in EV-71 viral genome that appear to attenuate the virus. The EV-A71 mutant VP1-E145G gave a yield of  $3.5 \times 10^5$  PFU/ml and the mutant VP1-244K produced a decrease in number of plaques ( $2.5 \times 10^5$  PFU/ml) in comparison to the EV-A71 wild type (5865/Sin/000009), although the plaque counts were higher than the mutant PD ( $1.0 \times 10^5$  PFU/mL). The mutant VP1-98E also showed reduced plaque number ( $7.5 \times 10^5$  PFU/mL). As there was reduction in viral growth, this was indicative that the plaque forming capability has been decreased markedly for several mutant strains. This signifies that there would be weaker viremia due to a reduction in viral copy number as viral load induces pathogenicity.

#### 4. Discussion

In our previous investigation, we genetically engineered the EV-A71 sub-genotype B4 (5865/Sin/000009) through site directed mutagenesis via the substitution of nt. at positions 475, 486, and 487 as these nts. were the molecular determinants of neurovirulence in PV Sabin strains 1, 2 and 3. We also introduced a partial deletant (PD) in the 5'-NTR region (deletion from nt. 475-485 in the 5'-NTR) as it may be genetically more stable than single site mutations. The study concluded that the EV-A71 partial deletant (PD) and mutant 475 demonstrated the lowest RNA copy number, plaques and VP1 protein followed by EV-A71

mutants 487, 5262, 158 and 486 in the order listed. This shows that the mutant PD could serve as a potential vaccine seed strain to carry beneficial mutations that will further attenuate or stabilize it to become a good LAV candidate (Yee et al., 2016).

In addition, better attenuated mutants could be constructed by introducing multiple mutations into the attenuated EV-A71 mutant PD. With advances in molecular biology, novel approaches to viral attenuation can be further studied such as altered replication fidelity and codon deoptimization. As for the latter approach, synonymous codons can be substituted all over a viral genome, hence preventing a decrease in immunogenicity and minimal possibility of reversion to wild type virulence. Studies on codon bias on viral multiplication and pathogenicity of poliovirus (PV) have been reported (Burns et al., 2009; Mueller et al., 2006). Interestingly, many studies have discovered that the deoptimized viruses remained attenuated after repeated passages and hence, were genetically stable with minimal risk of reversion. As both PV and EV-A71 share very high percentage of sequence homology hence, the codon deoptimization research on PV published in recent work could be referred to in the production of highly attenuated EV-A71 viruses. Therefore, we constructed several codon deoptimized EV-A71 viruses by substituting synonymous codon at positions VP1 (98E), VP1 (244K), VP1 (244K), VP2 (149K) and 2A (930K) to evaluate the effect of each codon deoptimization on replication fitness in Rhabdomyosarcoma (RD) cells.

Thus far, there is no quantification of the effects of different amino acids in the viral genome on virulence except for studies of comparison of nt. and amino acid sequences between virulent and non-virulent strains. In addition, most of the studies using comparative analysis between the strains were of sub-genotype C4. For example, 4 aa.

differences in the VP1 region (Gly<sup>P710</sup>/Gln<sup>P710</sup>/Arg<sup>P710</sup>/Glu<sup>P729</sup>), Lys<sup>P930</sup> in 2A region and 4 nts. in the 5'-NTR region (A<sup>P700</sup>/U<sup>P700</sup>, G<sup>P272</sup>, U<sup>P488</sup>) were found after aligning the VP1 sequences between fatal and mild EV-A71 strains (sub-genotype C4) (Li et al., 2011). These aa. demonstrate that there were several genetic determinants for virulent EV-A71 strains and these aa. could possibly be responsible in changing mild strains into fatal ones. This is to be expected as the 5'-NTR was responsible for cap-independent translation of viral proteins. As such, research reported in the study by Li et al. (2011) served as a reference to assess quantitatively the degree of attenuation of EV-A71 mutants constructed in this study to carry mutations C272U, U488C and U700C in the viral genome.

The importance of a C104U nt. substitution in the 5'-NTR region (between the cloverleaf and stem-loop II region) of CV-A16 was first demonstrated by Li et al. (2016). This mutation could significantly lower RNA replication and inhibit translational activity *in vitro* and also in the neonatal ICR mice. They identified that the nt. C104U could possibly be a molecular determinant of virulence for the lethal CV-A16 strain. The mutation affected the binding of the heterogeneous nuclear ribonucleoprotein K (hnRNP K) and A1 (hnRNP A1) with the 5'-NTR, hence reducing translational rates. This was discovered by aligning with nt. sequences in the 5'-NTR of the prototype G10, the non-lethal SHZH05 strains and the lethal Changchun024 strain. Thereby, the authors constructed infectious mutants of CV-A16 with different nt. substitutions in the 5'-NTR (Li et al., 2016). Similar to the finding that the 5'-NTR region is also carrying the specific genetic determinants for virulent EV-A71 sub-genotype C4 strains, this study reporting specific nt. changes in the 5'-NTR of CV-A16 with subsequent reductions in viral replication lends credence that the 5'-NTR region is a virulence-associated site.

In addition, Caine et al. (2016) discovered that a single mutation in VP1-244 (K244E) was crucial for mouse-adapted EV-A71 (mEV-A71) virulence and expanded tissue tropism in adult interferon-deficient AG129 mice. They also found a new VP1 mutation (H37R) that was important for K244E recovery in primate cell culture (Vero cells). The authors postulated that the H37R/K244E interaction is pertinent for replication in primate cells but the K244E mutant could replicate alone in a murine model (Caine et al., 2016). Three positions were demonstrated to be conserved among neurovirulent strains but were different from sub-genotype C4a strains carrying mild HFMD (Val<sup>P1148</sup>/Ile<sup>P1148</sup> in 3A, Val<sup>P814</sup>/Ile<sup>P814</sup> in VP1, Ala<sup>P1728</sup>/Cys<sup>P1728</sup>/Val<sup>P1728</sup> in 3C). These amino acid residues may be potential genetic determinants of virulence. Amongst all the 3 neurovirulent strains, SDLY107 varied in 4 nts. (C<sup>P579</sup>/T<sup>P579</sup>, C<sup>P241</sup>/T<sup>P241</sup>, A<sup>P571</sup>/T<sup>P571</sup> in 5'-NTR and T<sup>P7335</sup>/C<sup>P7335</sup> in 3'-NTR), suggesting that these nt(s). may be genetic determinants of virulence (Wen et al., 2013). Liu et al. (2014) discovered that there were 9 aa. differences in the VP1 sequences (E145G/Q, V249I, H22Q, P27S, N31S/D, E98K, D164E, T240A/S, A289T) in a comparison between fatal and mild EV-A71 strains (sub-genotype C4). These aa. could be possible genetic determinants of virulence in EV-A71 that could convert mild strains into fatal ones (Liu et al., 2014). The position of a single or a combination of aa. may have deep implications for virulence in different EV-A71 genotype/sub-genotype strains.

Wang et al. (2012) performed analysis on seven EV-A71 sequences (sub-genotype C4) from HFMD patients in Changchun, China who suffered either mild or severe HFMD. They identified that these seven viruses were actually recombinant viruses evolved from different type A Enteroviruses. For example, these viruses contained genetic recombination events between CV-A4, CV-A5, and EV-A71 (sub-genotypes B4 and C1) and hence not surprisingly, most of the structural protein, P1 of these viruses resembled that of the

prototype EV-A71, sub-genotype C1 strains. There was also a very high amount of similarity between the non-structural proteins (P2 and P3) and CV-A4, CV-A5, with EV-A71 (sub-genotype B4) in varying genomic regions possibly due to genomic recombination events. As our viral strain was also of sub-genotype B4, our working strain may have evolved from a single common ancestor that had continuously evolved over the years. This has serious implications as a virus that continuously undergoes genetic recombination could lead to the evolution of more virulent viruses. This would then make designing of a vaccine more difficult for such viruses that have high mutability rates (Wang et al., 2012). Hence, further studies such as phylogenetic analysis of isolates from mild/severe patients infected with EV-A71 (sub-genotype B4) should be carried out to determine the pattern of evolution.

Interestingly, when Threonine at position 251 within the 3D<sup>Pol</sup> region was substituted with Isoleucine (T251I), it altered the temperature susceptibility of EV-A71 (sub-genotype C2) from total susceptibility to complete resistance at 39.5°C *in vitro*. This strain also had increased viral virulence and showed clinical symptoms *in vivo* (Huang et al., 2015). The pathogenicity of mutant T251I was not evaluated in our investigation as the EV-A71 strain 41 (sub-genotype B4) does not carry a threonine (T) at residue 251 when compared to the sub-genotype C2 in the study conducted by Huang et al. (2015). However, we constructed a mutant similar to that of Meng and Kwang (2014) who produced highly attenuated EV-A71 mutants displaying high-fidelity with a single aa. change, (G64R) in its RdRP that greatly reduced pathogenicity *in vivo*. These EV-A71 mutants have lower pathogenicity as they are unable to generate replication-efficient mutations and have much lower genetic diversity to withstand a wide range of selective pressures. The authors postulate that the G64R mutant

could serve as a promising vaccine candidate as G64R mutant was genetically stable in the brain and muscle of infected mice at 12<sup>th</sup>-day post-infection (Meng and Kwang, 2014).

Kataoka et al. (2013) discovered that if glutamic acid (E) was present at aa. VP1-145 (sub-genotype C1), the virus induced neuro-pathogenesis and viremia more efficiently in cynomolgus monkeys than if glycine (G) was found at residue 145 (Kataoka et al., 2015). It was also demonstrated that the E145Q substitution within the VP1 region was a frequent change in the EV-A71 viral genomes of strains associated with mild and fatal HFMD cases. Generally, fatal strains had more substitutions in the IRES and 5'-NTR regions (Chang et al., 2012). This was of no surprise as these regions were responsible for receptor binding and translation of viral mRNA. The VP1-145 amino acid has been determined as a “hot spot” for evolutionary pressures on EV-A71 (Tee et al., 2010). In order to investigate the involvement of VP1-145 and G64R in the molecular basis of virulence in EV-A71 sub-genotype B4, site directed mutagenesis at positions G64R and VP1-E145G was conducted at these 2 sites to analyze the effects of both the mutations on virulence.

However, one of the disadvantages of a LAV would be its potential to revert back to wild type virulence, especially if the strain consists of “hot spots” for mutations. Hence, to boost the genetic stability of the LAV, multiple mutations were further introduced into the EV-A71 genome to reduce reversion and increase the stability of LAVs. The virulence of the different EV-A71 mutant strains was evaluated in the RD cell line by cytopathic effects, viral titer by tissue culture infectious dose (TCID<sub>50</sub>), plaque assays, detection of VP1 and real time determination of RNA copy number. After the effects brought about by each of the single site mutation and the partial deletion were quantified, the most significant mutations that could reduce virulence were selected and introduced into the PD mutant.

Hence, we had constructed a multiply mutated EV-A71 strain (MMS) by substituting six different nucleotides at U700C, VP1-E145G, VP1-242K, VP1-98E, VP1-244K, G64R (3D<sup>pol</sup>) in the strain carrying a partial deletant ( $\Delta$ 11bp) within the 5'-NTR region.

Very little VP1 quantity was observed in the EV-A71 mutants having site specific mutations at nt. 475 and 487 in the 5'-NTR. An examination of the TCID<sub>50</sub> values showed that the MMS needed significantly greater viral titer ( $3.16 \times 10^8$ ) to show CPE in 50% of the infected cells. This was to be expected as the MMS had lower infectivity in RD cells than the other codon deoptimized and SDM mutants. Significantly lower RNA copy numbers were obtained for 3 mutants (MMS, VP1-244K, VP1-E145G) at  $1.3 \times 10^2$ ,  $2.9 \times 10^2$ , and  $4.5 \times 10^2$ , respectively. Although the MMS could not totally eradicate viral replication, there was significant  $10^5$ -fold decrease in viral growth.

Subsequently, the number of plaques produced by the various mutant strains was examined in RD tissue culture by plaque assays. If the capability to form plaques is reduced, this would mean that viral growth is slower, thereby producing a lower PFU/ml value. For example, the mutant VP1-244K ( $2.5 \times 10^5$  PFU/mL) and mutant VP1-E145G showed significant decreases in plaque count ( $3.5 \times 10^5$  PFU/mL) in comparison to the EV-A71 wild type (strain 41) with  $8.0 \times 10^8$  PFU/mL. The lowest plaque count was formed by the MMS ( $1.2 \times 10^4$  PFU/mL) and mutant C475U ( $7.0 \times 10^4$  PFU/mL).

Some of the site directed mutations such as those introduced into sites at 475, 487, VP1-145, VP1-244 and a deletion in mutant PD were very effective in reducing cytopathic effects, RNA copy numbers, plaque count, VP1 amount and TCID<sub>50</sub>. By combining the beneficial mutations into a single vaccine strain, the MMS may serve as a potential LAV candidate for further evaluation by virulence testing *in vivo*. Attenuated strains with low



viral RNA copy number are possible good vaccine strains as they could not replicate fast enough to yield high viral load and cause destruction of the tissue cells. Slow replication could infer that the cells could still carry enough antigens to stimulate a good immune response.

## 5. Conclusions

This investigation has isolated and characterized several EV-A71 mutants with significant attenuation of viral virulence in Rhabdomyosarcoma cells. Better attenuated mutants could be constructed by introducing multiple mutations into the attenuated EV-A71 mutant PD. It was discovered that EV-A71 mutants carrying mutations at C272U, U488C and U700C in the 5'-NTR were not highly attenuated as they still produced more RNA, VP1 protein, plaque count and had lower TCID<sub>50</sub> values than other SDM and codon deoptimized mutants. Therefore, they are not significant virulence determinants for the wild type EV-A71 strain 41 (sub-genotype B4) in comparison to the sub-genotype C4 fatal strains studied by Li et al. (2011) (Li et al., 2011). The multiple mutations in the MMS did not totally eradicate the capability of the virus to multiply *in vitro*, but there were significant decreases in replication. Further studies should be conducted to investigate the stability of the MMS. A strain which is genetically highly stable and does not revert easily would thereby make a better LAV for EV-A71.

The results support the hypothesis that every EV-A71 genotype or sub-genotype carries a different virulence determinant or a combination of significant virulence determinants. In a particular sub-genotype, there may be several amino acids that determine virulence; hence it is important to identify significant amino acid residues that could be combined in the rational design of effective LAVs. Therefore, the results obtained in this study demonstrate

that quantifying the reduction of virulence through comparison of each SDM and partial deletion introduced into the genome is more effective than comparison of sequences between fatal and non-fatal strains.

### Acknowledgments

We are very appreciative of the support of the Fundamental Research Grant Scheme [FRGS/2/2014/ST03/SYUC/1]; Sunway University Internal Grants [INT-RRO-2014-017 and INT-VCO-0214-01] and the Sunway University Vice-Chancellor Fellowship to Isabel Yee. The grants funded the research consumables required for the execution of the project.

**Author Contributions:** PT Yee and CL Poh conceived and accomplished the project. PT Yee and CL Poh designed the experiments. Tan KO provided molecular biology advice and guidance. PT Yee performed the experiments. Tan KO and Ong SK provided critique to the article. PT Yee analyzed the data and prepared the article. All authors have read and approved the article.

**Conflicts of Interest:** All authors declare no conflict of interest.

### References

- Arita, M., Nagata, N., Iwata, N., Ami, Y., Suzaki, Y., Mizuta, K., Iwasaki, T., Sata, T., Wakita, T., Shimizu, H., 2007. An Attenuated Strain of Enterovirus 71 Belonging to Genotype A Showed a Broad Spectrum of Antigenicity with Attenuated Neurovirulence in Cynomolgus Monkeys. *J. Virol.* 81, 9386–9395.  
doi:10.1128/JVI.02856-06
- Buchan, J.R., Aucott, L.S., Stansfield, I., 2006. tRNA properties help shape codon pair

- 581 preferences in open reading frames. *Nucleic Acids Res.* 34, 1015–1027.  
582 doi:10.1093/nar/gkj488
- 583 Burns, C.C., Campagnoli, R., Shaw, J., Vincent, A., Jorba, J., Kew, O., 2009. Genetic  
584 Inactivation of Poliovirus Infectivity by Increasing the Frequencies of CpG and UpA  
585 Dinucleotides within and across Synonymous Capsid Region Codons. *J. Virol.* 83,  
586 9957–9969. doi:10.1128/JVI.00508-09
- 587 Burns, C.C., Shaw, J., Campagnoli, R., Jorba, J., Vincent, A., Quay, J., Kew, O., 2006.  
588 Modulation of Poliovirus Replicative Fitness in HeLa Cells by Deoptimization of  
589 Synonymous Codon Usage in the Capsid Region. *J. Virol.* 80, 3259–3272.  
590 doi:10.1128/JVI.80.7.3259-3272.2006
- 591 Caine, E.A., Moncla, L.H., Ronderos, M.D., Friedrich, T.C., Osorio, J.E., 2016. A Single  
592 Mutation in the VP1 of Enterovirus 71 Is Responsible for Increased Virulence and  
593 Neurotropism in Adult Interferon-Deficient Mice. *J. Virol.* 90, 8592–8604.  
594 doi:10.1128/JVI.01370-16
- 595 Chang, S.-C., Li, W.-C., Chen, G.-W., Tsao, K.-C., Huang, C.-G., Huang, Y.-C., Chiu, C.-  
596 H., Kuo, C.-Y., Tsai, K.-N., Shih, S.-R., Lin, T.-Y., 2012. Genetic characterization of  
597 enterovirus 71 isolated from patients with severe disease by comparative analysis of  
598 complete genomes. *J. Med. Virol.* 84, 931–939. doi:10.1002/jmv.23287

- 599 Chia, M.Y., Chung, W.Y., Chiang, P.S., Chien, Y.S., Ho, M.S., Lee, M.S., 2014.  
 600 Monitoring Antigenic Variations of Enterovirus 71: Implications for Virus  
 601 Surveillance and Vaccine Development. *PLoS Negl. Trop. Dis.* 8.  
 602 doi:10.1371/journal.pntd.0003044
- 603 Chong, P., Liu, C.C., Chow, Y.H., Chou, A.H., Klein, M., 2015. Review of enterovirus 71  
 604 vaccines. *Clin. Infect. Dis.* doi:10.1093/cid/ciu852
- 605 Chua, B.H., Phuektes, P., Sanders, S.A., Nicholls, P.K., McMinn, P.C., 2008. The  
 606 molecular basis of mouse adaptation by human enterovirus 71. *J. Gen. Virol.* 89,  
 607 1622–1632. doi:10.1099/vir.0.83676-0
- 608 Gutman, G.A., Hatfield, G.W., 1989. Nonrandom utilization of codon pairs in *Escherichia*  
 609 *coli*. *Proc. Natl. Acad. Sci.* 86, 3699–3703. doi:10.1073/pnas.86.10.3699
- 610 Han, J.-F., Cao, R.-Y., Tian, X., Yu, M., Qin, E.-D., Qin, C.-F., 2010. Producing infectious  
 611 enterovirus type 71 in a rapid strategy. *Virol. J.* 7, 116. doi:10.1186/1743-422X-7-116
- 612 Huang, M.L., Chiang, P.S., Chia, M.Y., Luo, S.T., Chang, L.Y., Lin, T.Y., Ho, M.S., Lee,  
 613 M.S., 2013. Cross-reactive neutralizing antibody responses to enterovirus 71  
 614 infections in young children: implications for vaccine development. *PLoS Negl Trop*  
 615 *Dis* 7, e2067. doi:10.1371/journal.pntd.0002067
- 616 Huang, S.-W., Tai, C.-H., Fonville, J.M., Lin, C.-H., Wang, S.-M., Liu, C.-C., Su, I.-J.,

- 617 Smith, D.J., Wang, J.-R., 2015. Mapping Enterovirus A71 Antigenic Determinants  
618 from Viral Evolution. *J. Virol.* 89, 11500–6. doi:10.1128/JVI.02035-15
- 619 Kataoka, C., Suzuki, T., Kotani, O., Iwata-Yoshikawa, N., Nagata, N., Ami, Y., Wakita, T.,  
620 Nishimura, Y., Shimizu, H., 2015. The Role of VP1 Amino Acid Residue 145 of  
621 Enterovirus 71 in Viral Fitness and Pathogenesis in a Cynomolgus Monkey Model.  
622 *PLoS Pathog.* 11. doi:10.1371/journal.ppat.1005033
- 623 Kawamura, N., Kohara, M., Abe, S., Komatsu, T., Tago, K., Arita, M., Nomoto, A., 1989.  
624 Determinants in the 5' noncoding region of poliovirus Sabin 1 RNA that influence the  
625 attenuation phenotype. *J. Virol.* 63, 1302–9.
- 626 Li, R., Zou, Q., Chen, L., Zhang, H., Wang, Y., 2011. Molecular analysis of virulent  
627 determinants of enterovirus 71. *PLoS One* 6. doi:10.1371/journal.pone.0026237
- 628 Li, Z., Liu, X., Wang, S., Li, J., Hou, M., Liu, G., Zhang, W., Yu, X.-F., 2016.  
629 Identification of a nucleotide in 5' untranslated region contributing to virus replication  
630 and virulence of Coxsackievirus A16. *Sci. Rep.* 6, 20839. doi:10.1038/srep20839
- 631 Liu, Y., Fu, C., Wu, S., Chen, X., Shi, Y., Zhou, B., Zhang, L., Zhang, F., Wang, Z., Zhang,  
632 Y., Fan, C., Han, S., Yin, J., Peng, B., Liu, W., He, X., 2014. A novel finding for  
633 enterovirus virulence from the capsid protein VP1 of EV71 circulating in mainland  
634 China. *Virus Genes* 48, 260–272. doi:10.1007/s11262-014-1035-2

- 635 Meng, T., Kwang, J., 2014. Attenuation of Human Enterovirus 71 High-Replication-  
 636 Fidelity Variants in AG129 Mice. *J. Virol.* 88, 5803–5815. doi:10.1128/JVI.00289-14
- 637 Mueller, S., Papamichail, D., Coleman, J.R., Skiena, S., Wimmer, E., 2006. Reduction of  
 638 the Rate of Poliovirus Protein Synthesis through Large-Scale Codon Deoptimization  
 639 Causes Attenuation of Viral Virulence by Lowering Specific Infectivity. *J. Virol.* 80,  
 640 9687–9696. doi:10.1128/JVI.00738-06
- 641 Nomoto, A., Omata, T., Toyoda, H., Kuge, S., Horie, H., Kataoka, Y., Genba, Y., Nakano,  
 642 Y., Imura, N., 1982. Complete nucleotide sequence of the attenuated poliovirus Sabin  
 643 1 strain genome. *Proc. Natl. Acad. Sci. U. S. A.* 79, 5793–5797.  
 644 doi:10.1073/pnas.79.19.5793
- 645 Sharp, P.M., Tuohy, T.M.F., Mosurski, K.R., 1986. Codon usage in yeast: Cluster analysis  
 646 clearly differentiates highly and lowly expressed genes. *Nucleic Acids Res.* 14, 5125–  
 647 5143. doi:10.1093/nar/14.13.5125
- 648 Tee, K.K., Lam, T.T.-Y., Chan, Y.F., Bible, J.M., Kamarulzaman, A., Tong, C.Y.W.,  
 649 Takebe, Y., Pybus, O.G., 2010. Evolutionary Genetics of Human Enterovirus 71:  
 650 Origin, Population Dynamics, Natural Selection, and Seasonal Periodicity of the VP1  
 651 Gene. *J. Virol.* 84, 3339–3350. doi:10.1128/JVI.01019-09
- 652 Wang, X., Zhu, C., Bao, W., Zhao, K., Niu, J., Yu, X.-F., Zhang, W., 2012.

---

Characterization of Full-Length Enterovirus 71 Strains from Severe and Mild Disease  
Patients in Northeastern China. PLoS One 7, e32405.  
doi:10.1371/journal.pone.0032405

Wen, H.L., Si, L.Y., Yuan, X.J., Hao, S.B., Gao, F., Chu, F.L., Sun, C.X., Wang, Z.Y.,  
2013. Complete genome sequencing and analysis of six enterovirus 71 strains with  
different clinical phenotypes. Virol J 10, 115. doi:10.1186/1743-422x-10-115

Westrop, G.D., Wareham, K.A., Evans, D.M., Dunn, G., Minor, P.D., Magrath, D.I., Taffs,  
F., Marsden, S., Skinner, M.A., Schild, G.C., 1989. Genetic basis of attenuation of the  
Sabin type 3 oral poliovirus vaccine. J. Virol. 63, 1338–44.

World Health Organization, 2016. Hand, foot, and mouth disease situation update number  
503.[http://www.wpro.who.int/emerging\\_diseases/hfmd\\_biweekly\\_20161018.pdf?ua=1](http://www.wpro.who.int/emerging_diseases/hfmd_biweekly_20161018.pdf?ua=1)  
(accessed 12.05.17).

Yee, P.T.I., Tan, K.O., Othman, I., Poh, C.L., 2016. Identification of molecular  
determinants of cell culture growth characteristics of Enterovirus 71. Virol. J. 13, 194.  
doi:10.1186/s12985-016-0645-9

**Table 1.** Cytopathic effects (CPE) caused by EV-A71 mutants and the positive control (wild type EV-A71 sub-genotype B4).

EV-A71 Mutants	CPE
C475U	+
A486G	+++
G487A	+
VP1-98E	++
VP1-242K	+++
VP1-244K	+
G64R (3D <sup>pol</sup> )	++
Partial Deletant (PD) 5'-NTR	+
VP1-E145G	+
VP2-149K	++++
2A-930K	++++
C272U	+++
U488C	+++
C700U	++
Multiple Mutant strain (MMS)	+
Positive control (wild type EV-A71)	+++++

RD cells were infected with EV-A71 mutants and the positive control (wild type EV-A71 sub-genotype B4) at a multiplicity of infection (MOI) of 0.1.



**Figure 1.** CPE by EV-A71 mutants (a) VP1-98E (b) VP1-242K (c) VP1-244K (d) G64R (e) PD (f) VP1-E145G (g) VP2-149K (h) 930K (2A) (i) C272U (j) U488C (k) C700U (l) Multiple Mutant strain (MMS) (m) C475U (n) A486G (o) G487A in RD cells compared with (p) uninfected RD cells (negative control) and (q) infected RD cells (positive control).

**Figure 2.** Logarithm Tissue Culture Infectious Dose 50 (Log TCID<sub>50</sub>) of EV-A71 mutants compared with the positive control (EV-A71 sub-genotype B4). The plate was placed at 37°C for up to 48h and observed daily for CPE. The TCID<sub>50</sub>/ml values are determined based on the Reed and Muench formula from at least three independent experiments.

**Figure 3.** Viral RNA copy number quantification. Transfection of infectious RNA of EV-A71 mutants into RD cells was carried out with Lipofectamine 3000 reagent with a MOI of 0.1. (+) control refers to wild type EV-A71 sub-genotype B4. (-) control refers to RD cells with no virus infection. The RNA copy number was calculated at 24h post-infection by TaqMan Real-Time PCR based on the average of at least three biological replicates. Error bars indicate the standard deviation  $\pm$  mean.

**Figure 4.** Western blot using monoclonal antibodies against VP1 as the primary antibody. The quantity of total proteins from EV-A71 and  $\beta$ -actin in each lane was 20  $\mu$ g. The lanes are as follows: lane M, molecular weight marker (from 10 - 250 kilodaltons), lane 1, Mutant G64R; lane 2, Mutant VP1-98E; lane 3, Mutant VP1-E145G; lane 4, Mutant U488C; lane 5, Mutant G487A; lane 6, MMS; lane 7, A486G; lane 8, C475U; lane 9, Mutant VP1-242K; lane 10, Mutant VP1-244K; lane 11, Mutant C272U; lane 12, Mutant U700C; lane 13, Mutant Partial Deletant (PD); lane 14, VP2-149K; lane 15, 2A-930K; lane 16, Positive control (EV-A71 strain 41); lane 17, Negative control (non-infected cells). The molecular weights of the VP1 protein and  $\beta$ -actin are 36 kDa and 42 kDa, respectively.

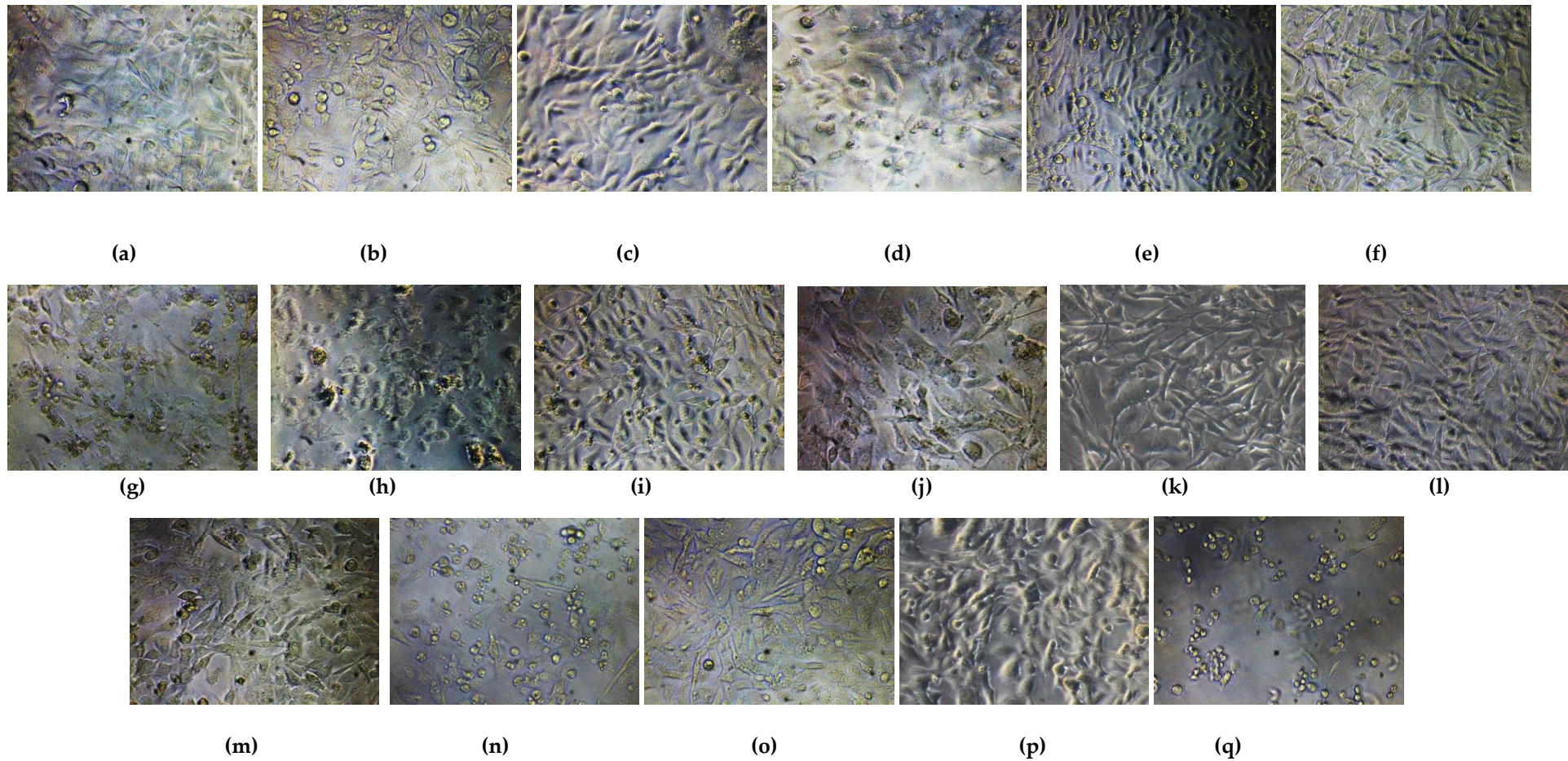
**Figure 5. Quantification of plaque counts by EV-A71 mutants and positive control (wild type EV-A71).** The plaque assays were carried out on RD cells incubated at 37°C for 48h from at least two independent experiments.

**Figure 6. Plaque Forming Units (PFU) by EV-A71 mutants in comparison with the positive control (wild type EV-A71).** RD cells were transfected with EV-A71 mutants and the positive control at a MOI of 0.1. Plaques were observed 48 h post-infection. PFU values are calculated based on the average of at least 2 biological replicates and error bars represent the standard deviation  $\pm$  mean.

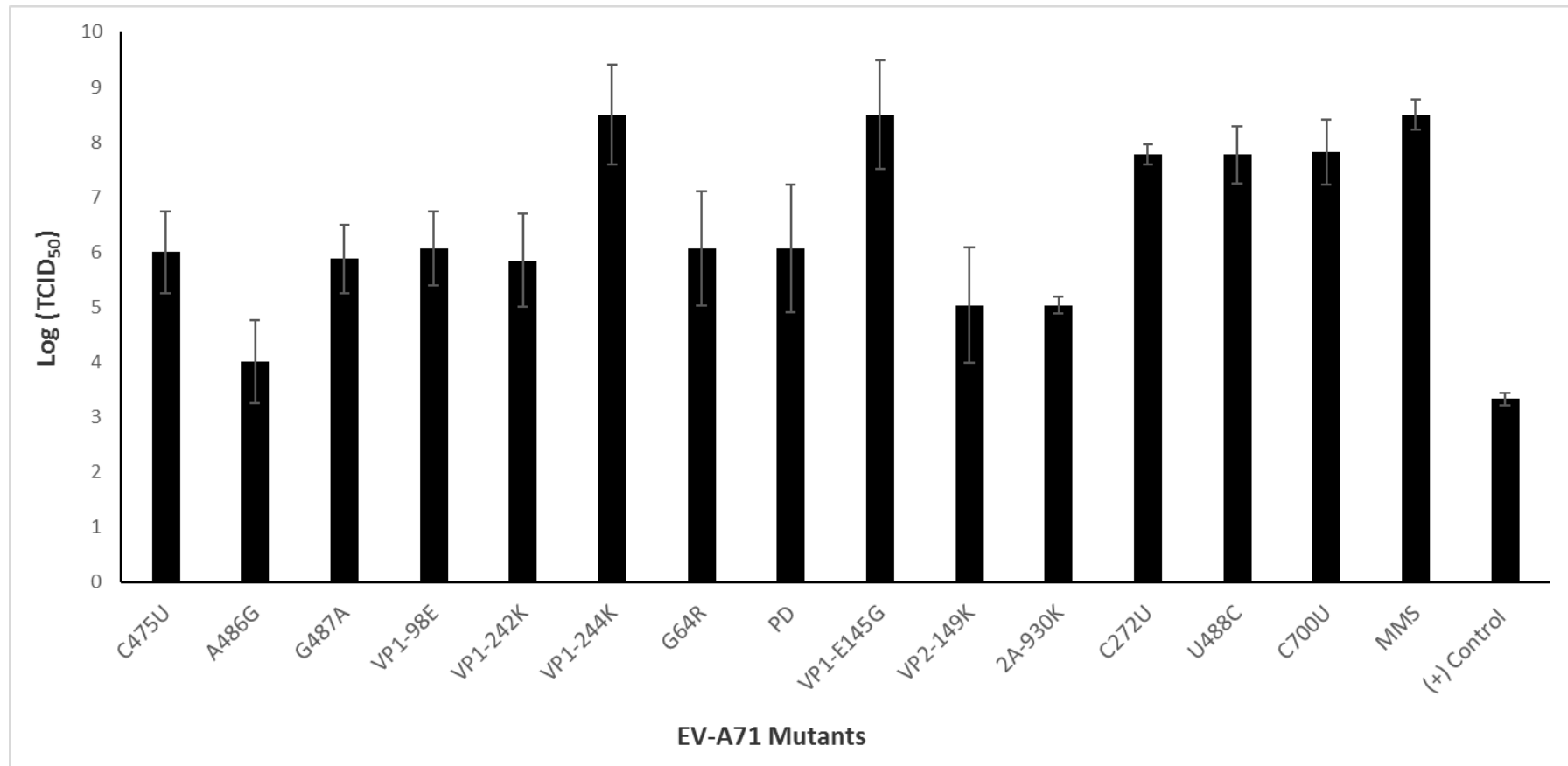
**Table 1.** Cytopathic effects (CPE) caused by EV-A71 mutants in comparison with the wild type EV-A71 strain 41.

EV-A71 Mutants	CPE
C475U	+
A486G	+++
G487A	+
VP1-98E	++
VP1-242K	+++
VP1-244K	+
G64R (3D <sup>pol</sup> )	++
Partial Deletant (PD) 5'-NTR	+
VP1-E145G	+
VP2-149K	++++
2A-930K	++++
C272U	+++
T488C	+++
C700U	++
Multiple Mutant strain (MMS)	+
Positive Control (EV-A71 strain 41)	+++++

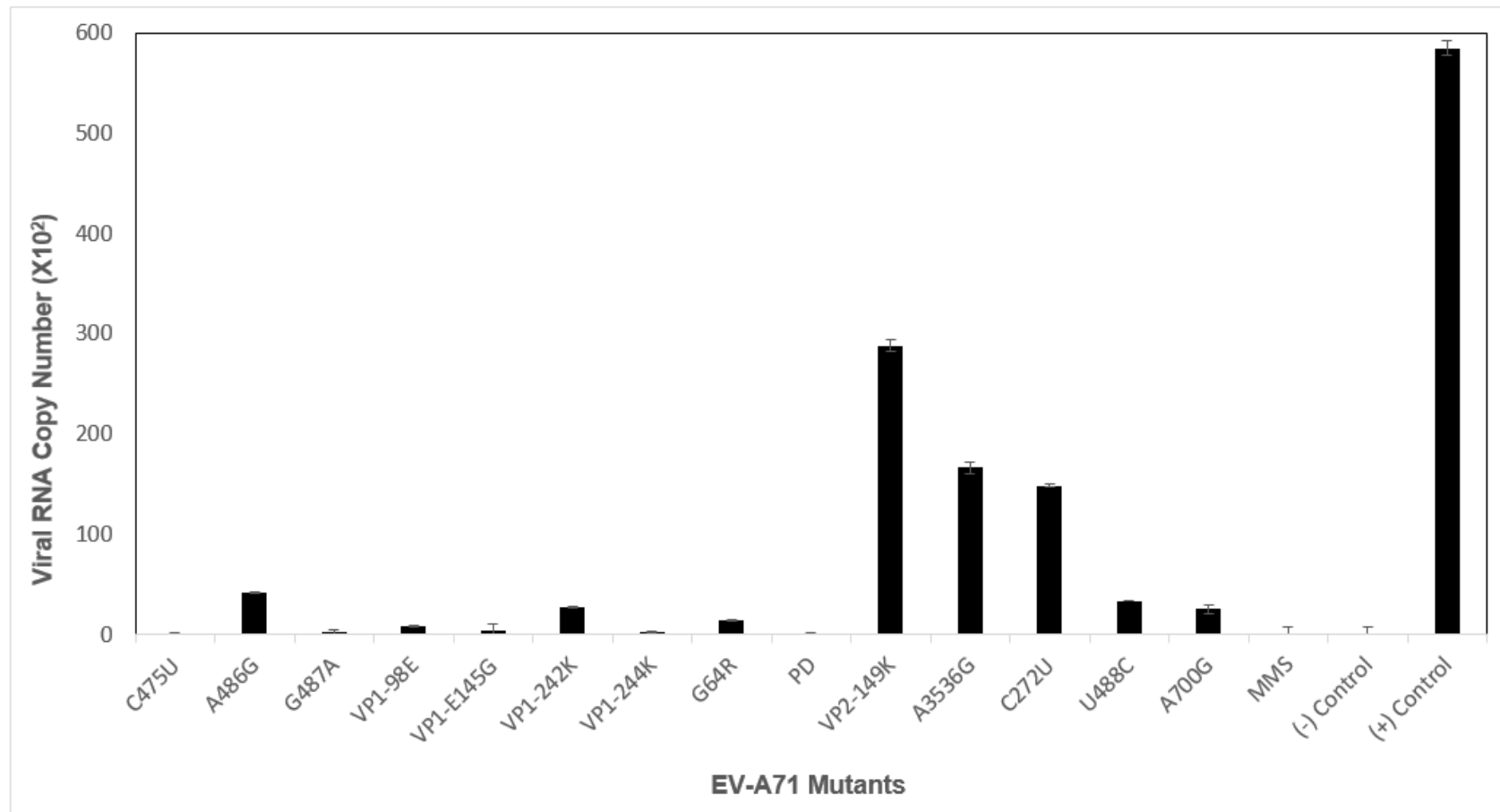
RD cells were infected with the EV-A71 wild type and mutant viruses at a MOI of 0.1. The TCID<sub>50</sub>/ml values are calculated using the Reed and Muench formula determined from three independent experiments.



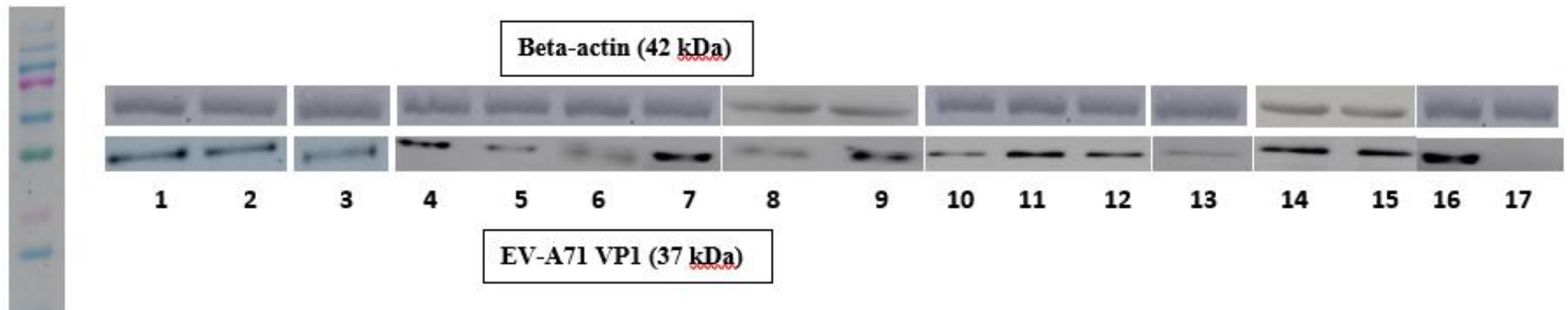
**Figure 1.** Cytopathic effects (CPE) caused by EV-A71 mutants (a) VP1-98E (b) VP1-242K (c) VP1-244K (d) G64R (e) PD (Partial Deletant 5'-NTR) (f) VP1-E145G (g) VP2-149K (h) 2A-930K (i) C272U (j) U488C (k) C700U (l) Multiple Mutant strain (MMS) (m) C475U (n) A486G (o) G487A in Rhabdomyosarcoma (RD) cells in comparison with (p) uninfected RD cells (negative control using Opti-MEM) and (q) EV-A71 wild type strain 41 infected RD cells (positive control).



**Figure 2.** Logarithm Tissue Culture Infectious Dose 50 (Log TCID<sub>50</sub>) of EV-A71 mutants in comparison with the wild type EV-A71 sub-genotype B4 strain 41. The plate was incubated at 37°C and observed daily for CPE up to 48h. The TCID<sub>50</sub>/ml values are calculated using the Reed and Muench formula determined from at least three independent experiments.

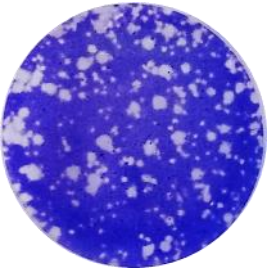
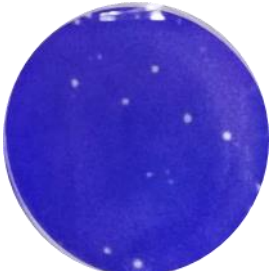



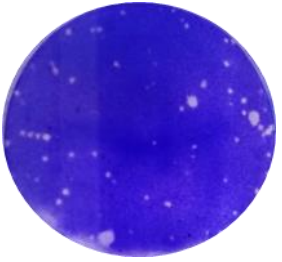
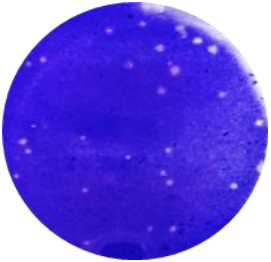
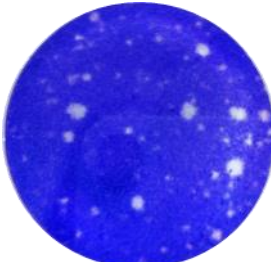
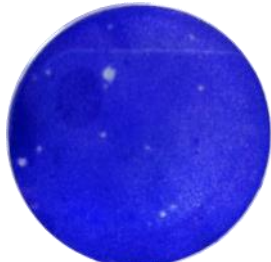




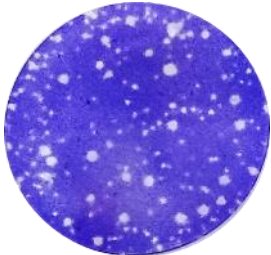
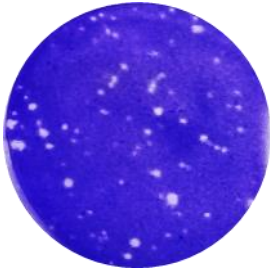

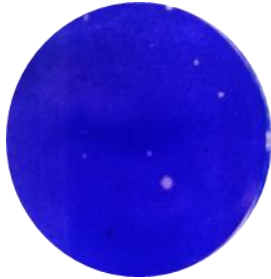
**Figure 3.** Quantification of Viral RNA Copy Number. Transfection of infectious RNA into RD cells was performed with the use of Lipofectamine 2000 reagent using EV-A71 mutants with a MOI of 0.1. (+) control refers to the EV-A71 sub-genotype B4 strain 41. (-) control refers to the RD cells with no virus infection. The viral RNA copy number was determined at 24h post-infection by TaqMan Real-Time PCR. Viral RNA copy numbers are the average of three biological replicates. Error bars represent the standard deviation of the mean.



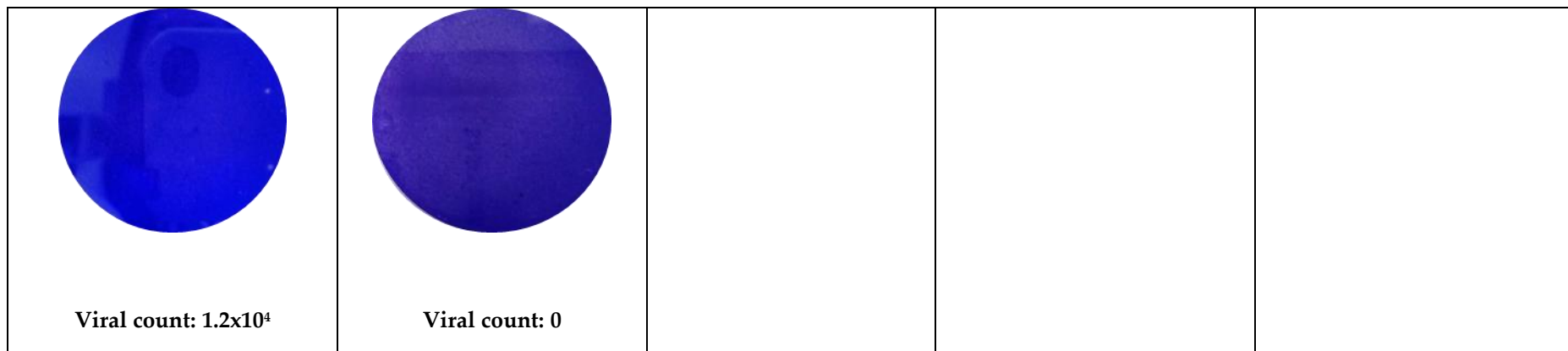
**Figure 4.** Western blot analysis using monoclonal antibody against VP1 as the primary antibody. The amount of EV-A71 total proteins and  $\beta$ -actin loaded in each lane was 20  $\mu$ g. The lanes are as follows: lane M, molecular weight marker (from 10 - 250 kilodaltons), lane 1, EV-A71 Mutant G64R; lane 2, Mutant VP1-98E; lane 3, Mutant VP1-E145G; lane 4, Mutant U488C; lane 5, Mutant G487A; lane 6, MMS; lane 7, A486G; lane 8, C475U; lane 9, Mutant VP1-242K; lane 10, Mutant VP1-244K; lane 11, Mutant C272U; lane 12, Mutant U700C; lane 13, Mutant Partial Deletant (PD); lane 14, VP2-149K; lane 15, 2A-930K; lane 16, Positive control (EV-A71 strain 41); lane 17, Negative control (uninfected RD cells). The molecular weights of the EV-A71 protein and  $\beta$ -actin are 36 kDa and 42 kDa, respectively.



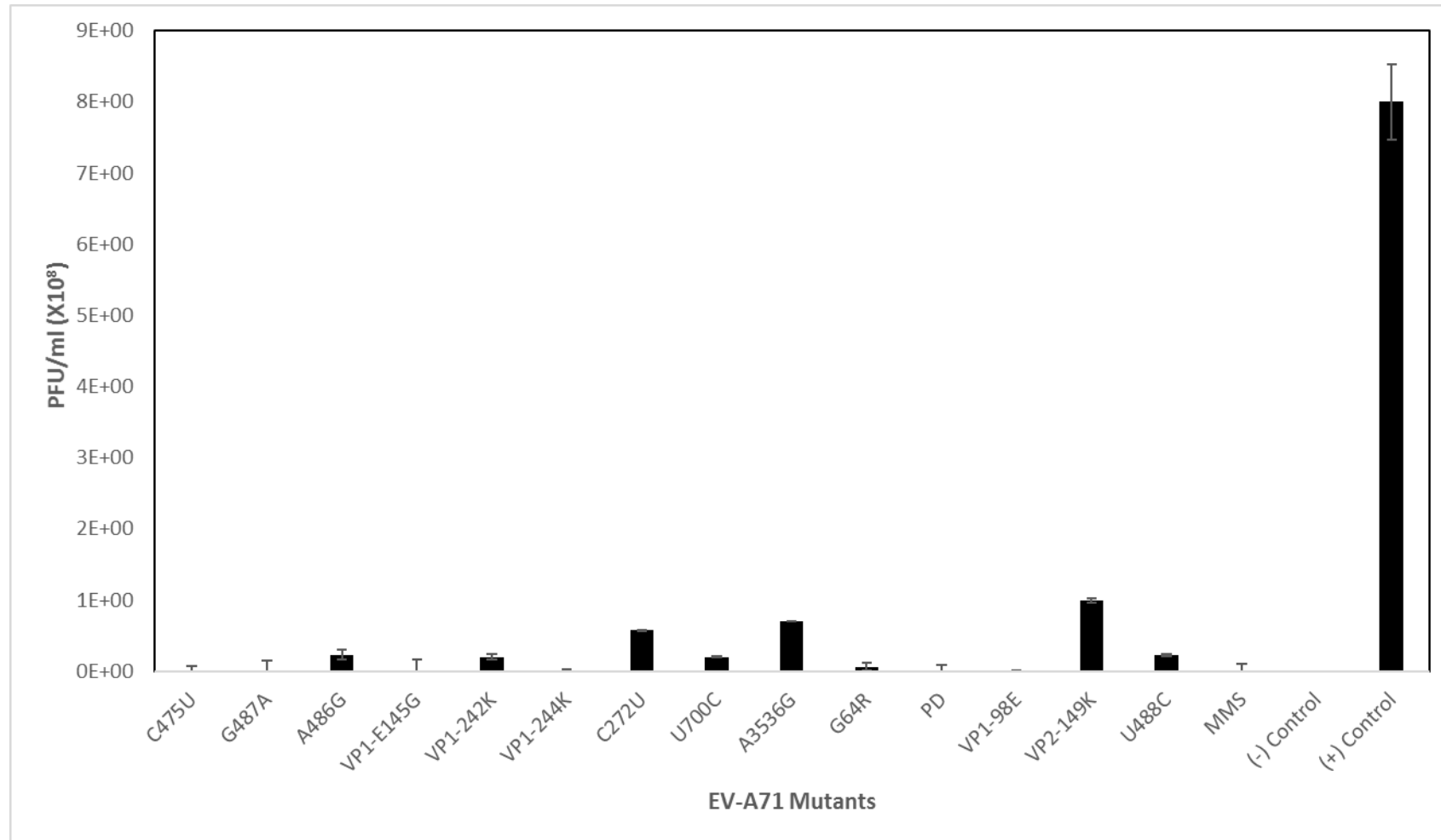
<p><b>(a) Positive control</b></p>  <p><b>Viral count: <math>8.0 \times 10^8</math></b></p>	<p><b>(b) VP1 (E145G)</b></p>  <p><b>Viral count: <math>3.5 \times 10^5</math></b></p>	<p><b>(c) 3D (G64R)</b></p>  <p><b>Viral count: <math>6.0 \times 10^6</math></b></p>	<p><b>(d) C475U</b></p>  <p><b>Viral count: <math>7.0 \times 10^4</math></b></p>	<p><b>(e) A486G</b></p>  <p><b>Viral count: <math>2.3 \times 10^7</math></b></p>
<p><b>(f) U488C</b></p>  <p><b>Viral count: <math>2.3 \times 10^7</math></b></p>	<p><b>(g) VP1-242K</b></p>  <p><b>Viral count: <math>2.0 \times 10^7</math></b></p>	<p><b>(h) C272U</b></p>  <p><b>Viral count: <math>5.7 \times 10^7</math></b></p>	<p><b>(i) VP1-244K</b></p>  <p><b>Viral count: <math>2.5 \times 10^5</math></b></p>	<p><b>(j) C700U</b></p>  <p><b>Viral count: <math>2.0 \times 10^7</math></b></p>

<p><b>(j) Partial Deletant (PD)</b></p>  <p><b>Viral count: <math>1.0 \times 10^5</math></b></p>	<p><b>(l) VP2-149K</b></p>  <p><b>Viral count: <math>9.9 \times 10^7</math></b></p>	<p><b>(m) 2A-930K</b></p>  <p><b>Viral count: <math>7.0 \times 10^7</math></b></p>	<p><b>(n) VP1-98E</b></p>  <p><b>Viral count: <math>7.5 \times 10^5</math></b></p>	<p><b>(o) G487A</b></p>  <p><b>Viral count: <math>1.4 \times 10^5</math></b></p>
<p><b>(p) MMS</b></p>	<p><b>(q) Negative control</b></p>			





**Figure 5. Quantification of plaque forming units by EV-A71 mutants and wild type EV-A71 strain 41.** The plaque assays were performed on monolayer RD cells incubated at 37°C and were repeated at least two separate times.



**Figure 6. Plaque Forming Units by EV-A71 mutants and the wild type EV-A71 strain 41.** RD cells were transfected with EV-A71 mutants and the wild type EV-A71 strain 41 at a MOI of 0.1. Plaque formation was observed 48 hours post-infection. PFU numbers are the average of two biological replicates; Error bars represent the standard deviation of the mean.